

Measurement of the Solar Neutrino Flux with an Array of Neutron Detectors in the Sudbury Neutrino Observatory

B. Jamieson (for the SNO collaboration)

University of British Columbia, Vancouver, BC V6T 1Z1, Canada

The Sudbury Neutrino Observatory has measured the ^8B solar neutrino flux using an array of ^3He proportional counters. Results obtained using a Markov-Chain Monte-Carlo (MCMC) parameter estimation, integrating over a standard extended likelihood, yield effective neutrino fluxes of: $\phi_{nc} = 5.54^{+0.33}_{-0.31}(\text{stat})^{+0.36}_{-0.34}(\text{syst}) \times 10^6 \text{ cm}^{-2}\text{s}^{-1}$, $\phi_{cc} = 1.67^{+0.05}_{-0.04}(\text{stat})^{+0.07}_{-0.08}(\text{syst}) \times 10^6 \text{ cm}^{-2}\text{s}^{-1}$, and $\phi_{es} = 1.77^{+0.24}_{-0.21}(\text{stat})^{+0.09}_{-0.10}(\text{syst}) \times 10^6 \text{ cm}^{-2}\text{s}^{-1}$. These measurements are in agreement with previous solar neutrino flux measurements, and with neutrino oscillation model results. Including these flux measurements in a global analysis of solar and reactor neutrino results yields an improved precision on the solar neutrino mixing angle of $\theta = 34.4^{+1.3}_{-1.2}$ degrees, and $\Delta m^2 = 7.59^{+0.19}_{-0.21} \text{ eV}^2$.

1. THE SNO DETECTOR

The Sudbury Neutrino Observatory (SNO) [1] is a low background neutrino detector ~ 2 km (6000 mwe overburden) underground in the Vale Inco Creighton nickel mine in Sudbury, Canada. The detector consists of 1000 tonnes of D_2O in a 12m diameter acrylic vessel surrounded by an inner shield of 1700 tonnes of H_2O . At the edge of the inner light water, a support structure holding about 9500 photomultiplier tubes (PMTs) provides 54% coverage. An additional outer shield of 5300 tonnes of light water surrounds the PMTs.

The SNO detector detects the neutrino reactions: $\nu_x + e^- \rightarrow \nu_x + e^-$ (ES), $\nu_e + d \rightarrow p + p + e^-$ (CC), and $\nu_x + d \rightarrow p + n + \nu_x$ (NC). The SNO detector provides the unique detection of the neutrons in the NC reaction by three different methods, one for each phase of SNO running. The first phase detected gamma rays from the triton production in the detector ($n + d \rightarrow t + \gamma + 6.25 \text{ MeV}$)[2]. In SNO's second phase NaCl was added to the heavy water, and increased the neutron capture through neutron capture on the Cl ($n + ^{35}\text{Cl} \rightarrow ^{36}\text{Cl} + \gamma + 8.6 \text{ MeV}$), where the 8.6 MeV is the sum of a cascade of gamma rays[3].

For the final phase of SNO reported on here the neutron is detected when it is captured in an array of 36 ^3He proportional counters (NCDs) via the reaction $n + ^3\text{He} \rightarrow p + t + 0.76 \text{ MeV}$ [4][5]. The NCD phase measurement separates the NC and CC signal detection which significantly reduces the CC spectrum contamination by the 6.25 MeV neutron captures on deuterium. The NCD phase is more complex however since $\sim 10\%$ of the Cherenkov light is blocked by the array, the radioactivity of the counters adds a non-negligible background, and the signal rate of ~ 1000 neutrons/year is fairly low.

2. NCD DETECTOR ENERGY SPECTRUM CALIBRATION

The neutron energy spectrum is measured with calibration data from a $^{24}\text{NaCl}$ brine that produces neutrons by the gamma capture on deuterium ($\gamma + d \rightarrow p + n$). The spectrum is characterized by a peak at 0.76 MeV with features at 0.57 MeV and 0.19 MeV where either only the proton or triton are seen in the proportional counter.

The $^{24}\text{NaCl}$ brine is the calibration source most like the neutrons produced from solar neutrinos since it can be uniformly distributed in the D_2O , and it also provides a measurement of the neutron detection efficiency (0.211 ± 0.007). The mixing of the brine can be seen by looking at the light output from different parts of the detector, and only data from after the brine was uniformly mixed was used. In addition, the detection efficiency from the MCNP [6] Monte Carlo code yielded an efficiency of 0.210(3). Finally a time-series based analysis using neutron bursts from a ^{252}Cf source confirmed these neutron efficiency measurements.

A simulation of the NCD detector was used to model the energy spectrum from background alphas from U, Th, and Po in the nickel of the NCD walls. The model included effects of the energy loss, multiple scattering, electron-ion pair

generation, electron drift and diffusion, electron multiple scattering, ion mobility, electron avalanche, space charge, signal generation, and a detailed propagation through the electronics. The Monte Carlo simulation was tuned for the surface to bulk alpha ratio, energy scale, energy resolution, alpha depth, and contributions from different parts of the NCD using the alphas above 2 MeV. The simulation was found to reproduce the pulse width and energy spectrum very well, including the effects of alphas from the NCD anode wires.

Instrumental events in the NCD detector were easily separated from ionization events using an amplitude versus energy cut. Six of the 36 NCD strings with high instrumental rates were removed from the analysis. Two probability distribution functions for the instrumental backgrounds were included in the signal-extraction to fit for an unconstrained number of instrumental events.

3. BLIND ANALYSIS

Three blindfolds were implemented on the NCD phase measurement. One month of the data was open for analysts to tune cuts. A hidden fraction of neutrons that follow muons were added to the data, and an unknown fraction of candidate events were omitted. Detailed internal documentation was reviewed by topic committees before the box was opened to reveal the true solar neutrino flux measurement.

The box was opened on May 2, 2008, and the results are presented as found after correcting two inconsistencies. The three separate signal-extraction codes had to correct pilot errors on the inputs to the final fit, which resulted in no change in the central values, and made the final uncertainties reported agree. An incorrect algorithm in fitting the peak value of the ES posterior distribution was replaced.

4. NEUTRON BACKGROUNDS

The neutron backgrounds were measured for the D₂O radioactivity, atmospheric neutrinos, ¹⁶N neutrons, NCD counter neutrons from the bulk of the counters, from hot-spots on the counters, and from the NCD cables. In addition, backgrounds from the acrylic-vessel, reactor neutrinos, and other sources were included in the background estimates. The neutron backgrounds are summarized in the following Table, and were included in the signal extraction broadening the uncertainties in the measured solar neutrino fluxes.

Table I: Table of neutron backgrounds in the PMT and NCD data.

Source	PMT neutrons	NCD neutrons
D ₂ O radioactivity	7.6±1.2	28.7±4.7
Atmospheric ν , ¹⁶ N	24.7±4.6	13.6±2.7
Other backgrounds	0.7±0.1	2.3±0.3
NCD bulk PD, ^{17,18} O(α ,n)	4.6 ^{+2.1} _{-1.6}	27.6 ^{+12.9} _{-10.3}
NCD hot-spots	17.7±1.8	64.4±6.4
NCD cables	1.1±1.0	8.0±5.2
External-source neutrons	20.6±10.4	40.9±20.6
Total	77 ⁺¹² ₋₁₀	185 ⁺²⁵ ₋₂₂

5. SIGNAL EXTRACTION METHODS

Parameter estimation, and estimation of the uncertainties on all fit parameters (both fluxes and nuisance parameters for systematics) is done with a Metropolis algorithm Markov-Chain Monte Carlo (MCMC)[7].

In SNO's previous signal extractions, the negative log-likelihood (NLL) function was simply minimized with respect to all parameters to get the best-fit value, and the curvature of $-\log(L)$ at the minimum was used to determine the uncertainties. The floating systematics approach also uses a minimization, although with additional nuisance parameters added to account for systematic uncertainties.

Minimizing the NLL is very challenging for the 27 flux parameters ($\phi_{nc}, \phi_{cc1...13}, \phi_{es1...13}$) and 35 systematic parameters in the fit. The systematic parameters include PMT reconstruction uncertainties estimated from calibration data [8], both PMT and NCD efficiencies, NCD Monte Carlo and NCD instrumental uncertainties. In addition because the likelihood function can be a bit choppy near the minimum, traditional minimizers such as MINUIT run into trouble and often will not converge in reasonable periods of time.

The MCMC method gets around this problem by interpreting NLL as the negative log of a joint probability distribution for all of the free parameters. We then integrate over all nuisance parameters to determine the distributions for the fluxes. The origins of this procedure go back to Bayesian probability theory, and in fact our approach could be considered to be a Bayesian analysis with uniform priors assumed for the fluxes.

The advantages of the MCMC method are twofold. First, it converges much faster than a 50+ parameter MINUIT minimization. Rather than minimizing over parameters, we in fact integrate over nuisance parameters. Second, since we integrate over nuisance parameters with the MCMC instead of trying to find a best-fit point, we are insensitive to and in fact average over choppiness in the NLL that would interfere with finding a minimum. Both the speed of convergence and the insensitivity to numerical noise in the NLL means that the MCMC method is better suited to handling large numbers of nuisance parameters.

6. RESULTS

The final corrected solar neutrino fluxes above a 6 MeV Kinetic Energy threshold from the unblinded NCD data are: $\phi_{nc} = 5.54_{-0.46}^{+0.48} \times 10^6 \text{ cm}^{-2}\text{s}^{-1}$, $\phi_{cc} = 1.67_{-0.09}^{+0.08} \times 10^6 \text{ cm}^{-2}\text{s}^{-1}$, and $\phi_{es} = 1.77_{-0.23}^{+0.26} \times 10^6 \text{ cm}^{-2}\text{s}^{-1}$. The correlation between ϕ_{cc} and ϕ_{nc} was only -0.19 in the NCD phase fit including all systematic uncertainties. The ϕ_{es} is a 2.2 sigma lower than the Super Kamiokande measurement, but the full set of fluxes has a probability of 32.8% of being consistent with the six other flux measurements from all of the SNO phases.

The NCD energy fit, unconstrained PMT energy fit, PMT angle to the Sun, and radial position fits are shown in FIG. 1. It can be seen in the PMT energy fit that the number of neutrons in the PMT is considerably less than either the SNO D₂O or salt phases, and provides the better CC separation than in those phases.

Including the NCD phase flux measurements in a global oscillation analysis results in an improved precision on the solar neutrino mixing angle of $\theta = 34.4_{-1.2}^{+1.3}$ degrees, and $\Delta m^2 = 7.59_{-0.21}^{+0.19} eV^2$.

Acknowledgments

SNO gratefully acknowledges NSERC, Industry Canada, NRC, Northern Ontario Heritage Fund, Vale INCO, Atomic Energy of Canada, Ontario Power Generation, High Performance Computing Virtual Laboratory, Canada Foundation for Innovation, Canada Research Chairs, Westgrid, US Department of Energy, NERSC PDSF, UK STFC, and Portugal FCT.

References

- [1] SNO Collaboration, Nucl. Instrum. and Methods Phys. Res., Sect. A **449**, (2000) 172.
- [2] SNO Collaboration, Phys. Rev. Lett. **87**, (2001) 071301. SNO Collaboration, Phys. Rev. Lett. **89**, (2002) 011301. SNO Collaboration, Phys. Rev. Lett. **89**, (2002) 011302.

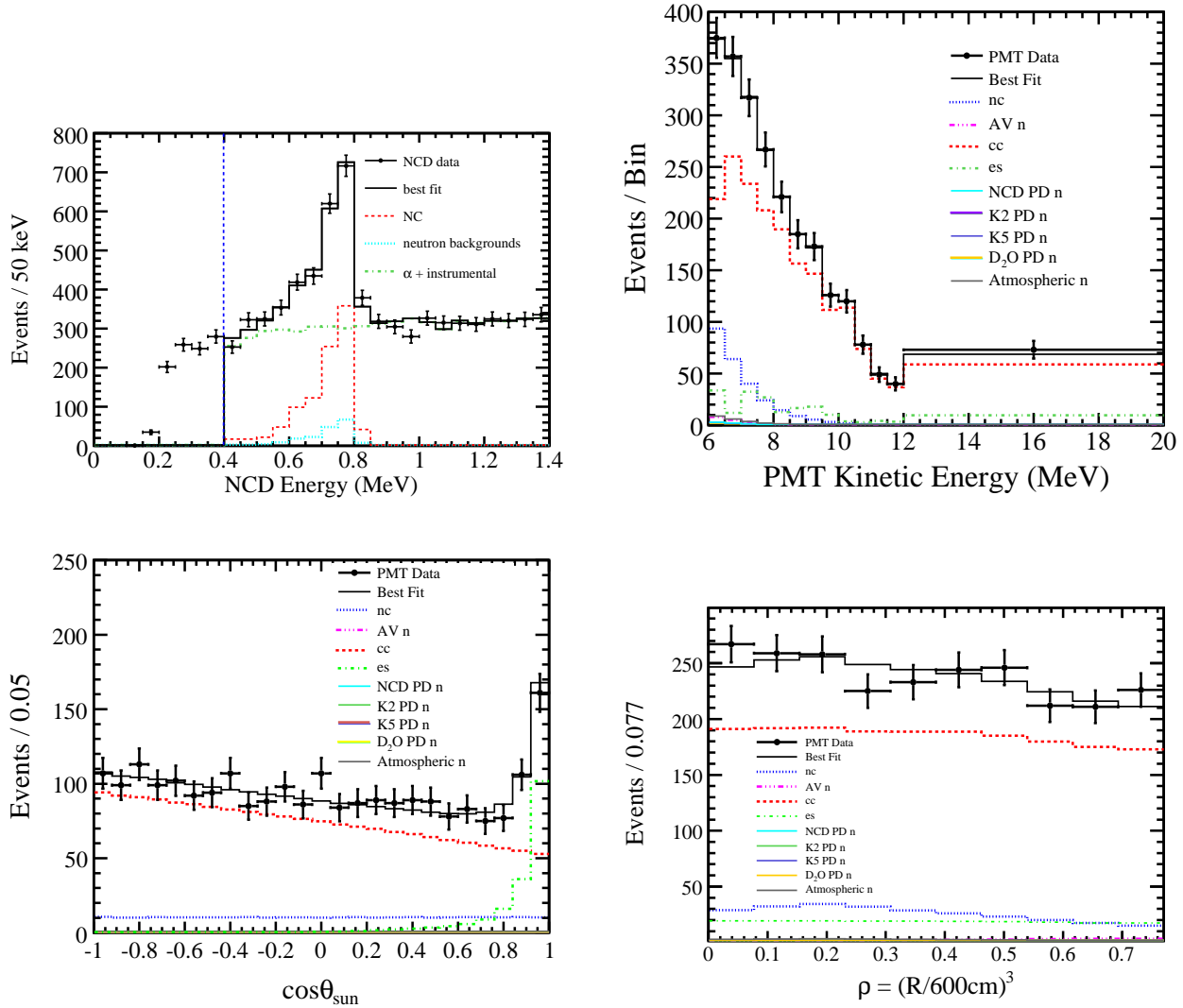


Figure 1: These figures show the NCD energy spectrum fit (top left), the PMT energy unconstrained fit (top right), the PMT angle to the sun fit (bottom left), and the PMT radial position fit (bottom right).

- [3] SNO Collaboration, Phys. Rev. Lett. **92**, (2004) 181301. Phys. Rev. **C72**, (2005) 055502. SNO Collaboration, Phys. Rev. **C75**, (2007) 045502.
- [4] J.F. Amsbaugh *et al.*, Nucl. Instrum. and Methods Phys. Res., Sect. A **579**, (2007) 1054.
- [5] SNO Collaboration, Phys. Rev. Lett. **101**, (2008) 111301.
- [6] Refer to the MCNP website for details:
http://mcnp-green.lanl.gov/publication/mcnp_publications.html
- [7] Metropolis *et al.*, Journ. Chem. Phys. **21**,(1953) 1087. W.K. Hastings, Biometrika **57**, (1970) 97.
- [8] M.R. Dragowsky *et al.*, Nucl. Instrum. and Methods Phys. Res., Sect. A **481**, (2002) 284. I. Blevis *et al.*, Nucl. Instrum. and Methods Phys. Res., Sect. A **517**, (2004) 139.